

Enhanced pyroelectric properties of $\text{Ca}_x(\text{Sr}_{0.5}\text{Ba}_{0.5})_{1-x}\text{Nb}_2\text{O}_6$ lead-free ceramics

Jing Zhang, Xianlin Dong, Fei Cao, Shaobo Guo, and Genshui Wang

Citation: [Applied Physics Letters](#) **102**, 102908 (2013); doi: 10.1063/1.4795795

View online: <http://dx.doi.org/10.1063/1.4795795>

View Table of Contents: <http://scitation.aip.org/content/aip/journal/apl/102/10?ver=pdfcov>

Published by the [AIP Publishing](#)

Articles you may be interested in

[Giant electrocaloric effect in lead-free \$\text{Ba}_{0.94}\text{Ca}_{0.06}\text{Ti}_{1-x}\text{Sn}_x\text{O}_3\$ ceramics with tunable Curie temperature](#)

Appl. Phys. Lett. **107**, 252905 (2015); 10.1063/1.4938134

[Tuning of dielectric, pyroelectric and ferroelectric properties of \$0.715\text{Bi}_{0.5}\text{Na}_{0.5}\text{TiO}_3\text{-}0.065\text{BaTiO}_3\text{-}0.22\text{SrTiO}_3\$ ceramic by internal clamping](#)

AIP Advances **5**, 087145 (2015); 10.1063/1.4929328

[Lead-free \$\text{Ba}_{0.8}\text{Ca}_{0.2}\(\text{Zr}_x\text{Ti}_{1-x}\)\text{O}_3\$ ceramics with large electrocaloric effect](#)

Appl. Phys. Lett. **106**, 042902 (2015); 10.1063/1.4906864

[Electro-caloric effect in \$\(\text{Ba}_{1-x}\text{Ca}_x\)\(\text{Zr}_{0.05}\text{Ti}_{0.95}\)\text{O}_3\$: A lead-free ferroelectric material](#)

Appl. Phys. Lett. **103**, 202903 (2013); 10.1063/1.4829635

[Optimized electrocaloric refrigeration capacity in lead-free \$\(1-x\)\text{BaZr}_{0.2}\text{Ti}_{0.8}\text{O}_3\text{-}x\text{Ba}_{0.7}\text{Ca}_{0.3}\text{TiO}_3\$ ceramics](#)

Appl. Phys. Lett. **102**, 252904 (2013); 10.1063/1.4810916

The banner features a blue background with a molecular structure of spheres and sticks on the left. On the right, the text 'NEW Special Topic Sections' is written in large, white, sans-serif font. Below this, the text 'NOW ONLINE' is in yellow, followed by 'Lithium Niobate Properties and Applications: Reviews of Emerging Trends' in white. The AIP Applied Physics Reviews logo is in the bottom right corner.

NEW Special Topic Sections

NOW ONLINE
Lithium Niobate Properties and Applications:
Reviews of Emerging Trends

AIP Applied Physics Reviews

Enhanced pyroelectric properties of $\text{Ca}_x(\text{Sr}_{0.5}\text{Ba}_{0.5})_{1-x}\text{Nb}_2\text{O}_6$ lead-free ceramics

Jing Zhang, Xianlin Dong, Fei Cao, Shaobo Guo, and Genshui Wang^{a)}

Key Laboratory of Inorganic Functional Materials and Devices, Shanghai Institute of Ceramics, Chinese Academy of Sciences, 1295 Dingxi Road, Shanghai 200050, People's Republic of China

(Received 23 January 2013; accepted 6 March 2013; published online 15 March 2013)

$\text{Ca}_x(\text{Sr}_{0.5}\text{Ba}_{0.5})_{1-x}\text{Nb}_2\text{O}_6$ [CSBN(x), $x = 0.00, 0.10, 0.15$, and 0.20] lead-free ceramics were prepared by a traditional solid-state reaction technique. Dielectric, ferroelectric, and pyroelectric properties of CSBN(x) lead-free ceramics were systematically investigated. The pyroelectric properties of CSBN(x) have been enhanced remarkably due to Ca addition and reached the maximum values at $x = 0.15$, with pyroelectric coefficient of $3.61 \times 10^{-8} \text{ C/cm}^2 \text{ K}$ and pyroelectric figure of merit of $F_i = 172 \text{ pm/V}$, $F_v = 0.021 \text{ m}^2/\text{C}$, and $F_d = 11.5 \mu\text{Pa}^{-1/2}$, which are superior to other lead-free ferroelectric ceramics. These results indicate the potential of CSBN(x) ceramics for infrared detector applications. © 2013 American Institute of Physics.
[\[http://dx.doi.org/10.1063/1.4795795\]](http://dx.doi.org/10.1063/1.4795795)

Pyroelectric infrared detectors have been of interest for many years because of their broad wavelength response, good sensitivity, and high stability over a wide temperature range.^{1–3} Ferroelectric ceramics widely used in pyroelectric infrared detectors are mainly lead-based ceramics.^{4,5} However, considering the toxicity of lead and its compounds, there is a general awareness for the development of environmental friendly lead-free pyroelectric materials.

Therefore, several systems of lead-free ceramics such as $\text{Bi}_x\text{Na}_{1-x}\text{TiO}_3$ (BNT),^{6,7} $\text{K}_{1-x}\text{Na}_x\text{NbO}_3$ (KNN),⁸ and $\text{Sr}_{1-x}\text{Ba}_x\text{Nb}_2\text{O}_6$ (SBN)^{9–11} have been developed for pyroelectric applications. Among them SBN have been reported to exhibit high pyroelectric coefficient of $5.5 \times 10^{-8} \text{ C/cm}^2 \text{ K}$ and $4.1 \times 10^{-8} \text{ C/cm}^2 \text{ K}$ in crystals⁹ and textured ceramics,¹⁰ respectively, which are comparable to lead zirconate titanate (PZT) ceramics. However, conventional sintered SBN ceramics have relatively low pyroelectric properties ($\sim 2 \times 10^{-8} \text{ C/cm}^2 \text{ K}$) due to their random orientation.¹²

Several dopants have been introduced to modify dielectric and pyroelectric properties of SBN, such as Cr, K, Na, Ca, and rare earth.^{13–15} Xie *et al.*¹⁶ found Ca-substitution to be capable of improving the ferroelectric properties of $\text{Sr}_{2-x}\text{Ca}_x\text{NaNb}_5\text{O}_{15}$ (SCNN) ceramics. Moreover, results reported by Yao *et al.*¹⁷ also revealed that the piezoelectric and pyroelectric performances of $(\text{Sr}_{0.6}\text{Ba}_{0.4})_4\text{Na}_2\text{Nb}_{10}\text{O}_{30}$ (SBNN) ceramics were enhanced by the Ca-dopant. In fact, $\text{Ca}_{0.28}\text{Ba}_{0.72}\text{Nb}_2\text{O}_6$ (CBN) crystal can exhibit higher spontaneous polarization ($35.3 \mu\text{C/cm}^2$)¹⁸ than SBN crystal ($27\text{--}32 \mu\text{C/cm}^2$).¹⁹ Hence it is anticipated that Ca-substitution could be an effective way to enhance the pyroelectric properties of SBN, yet no relevant work has been reported. In this letter, effects of Ca content on the structure and electric properties of $\text{Ca}_x(\text{Sr}_{0.5}\text{Ba}_{0.5})_{1-x}\text{Nb}_2\text{O}_6$ [CSBN(x), $x = 0.00, 0.10, 0.15$, and 0.20] ceramics are investigated. Enhanced ferroelectric and pyroelectric performances are obtained in CSBN(x) due to Ca-substitution, indicating its potential for applications in infrared detectors.

The CSBN(x) ceramics were prepared by a traditional solid-state ceramic fabrication method. Reagent grade BaCO_3 (99%), SrCO_3 (99%), CaCO_3 (99%), and Nb_2O_5 (99.5%) powders are used as starting raw materials, and all samples were sintered in air at 1350°C for 3 h. The crystal structure of the ceramics was characterized by X-ray diffraction (XRD, D/MAX-2550V; Rigaku, Tokyo, Japan) on sintered disks. The microstructure of the ceramics was taken by field emission scanning electron microscope (FESEM, S-4800, Hitachi, Japan) on the polished and heat-etched sample surface.

Electric measurements were carried out after the samples were coated with silver electrode on both sides. The dielectric constant (ϵ_r) and dissipation factor ($\tan \delta$) of poled samples were measured using a Hewlett Packard LCR meter at different frequencies in a temperature range from 20°C to 200°C . The polarization versus electric field (P - E) hysteresis loops were characterized by aixACCT TF Analyzer 2000 (aixACCT Systems GmbH; Dennewartstrasse, Aachen, Germany) with high-voltage power supply (Trek Inc., Medina, NY). A sinusoidal waveform was chosen for the electric field cycle. The pyroelectric properties were studied with a Keithley 6517A electrometer/high resistance meter for polarized samples. According to the P - E hysteresis loops and the poling progress reported for SBN,¹⁰ the samples were polarized in silicone oil under an electric field of 5 kV/mm at 150°C for 60 min and then cooled down until 40°C with the electric field maintained at 5 kV/mm .

Figure 1(a) shows the XRD patterns of CSBN(x) ceramics. The patterns indicate that all samples are crystallized into a pure tetragonal tungsten bronze (TTB) structure with no second phase being detected. Obvious splits and shifts of peaks can be noticed in the Ca-substituted samples, as shown in the partly enlarged patterns in Figure 1(b). The results suggested that the lattice constant decreases, and orthorhombic phases maybe appear due to the addition of CaNb_2O_6 (CN).²⁰ Figure 1(c) illustrates the surface microstructures of CSBN ceramics. The specimens are observed to exhibit dense structure with an average grain size of about $2 \mu\text{m}$.

The dielectric constant (ϵ_r) and dielectric loss ($\tan \delta$) of poled CSBN(x) ceramics as a function of temperature

^{a)}Electronic mail: genshuiwang@mail.sic.ac.cn

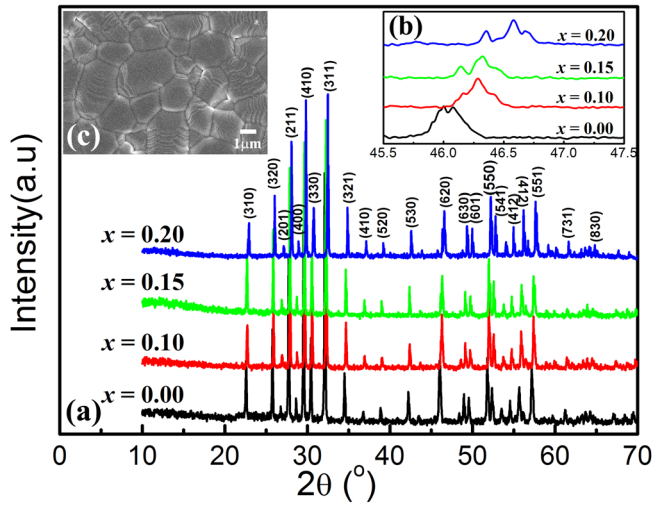


FIG. 1. (a) The X-ray diffraction patterns of CSBN(x) ceramics. (b) The magnification of XRD patterns in the 2θ range of $45.5\text{--}47.5^\circ$. (c) SEM micrographs of CSBN(0.15) ceramics.

measured at 1 kHz are depicted in Figure 2. The transition temperatures (T_c) of CSBN(x) ceramics are all around 90°C and change little as x increases. Diffuse phase transition (DPT) was discovered in all CSBN(x) samples. The considerable broadening of the phase transition with higher Ca content may be due to enhanced structural disorder and compositional fluctuations¹³ when smaller Ca^{2+} (0.99 \AA) substitutes Sr^{2+} (1.13 \AA) and Ba^{2+} (1.35 \AA) in A site.

Figure 3 shows the temperature-dependent pyroelectric coefficient (p) of CSBN(x) ceramics. Broad and gentle peaks are observed for all samples as a result of diffuse ferroelectric to paraelectric phase transition. The values of pyroelectric coefficient p at room temperature and volume specific heat c_v for CSBN(x) ceramics are listed in Table I. Besides, the figures of merit (FOM) related to the performance of the pyroelectric materials have been calculated.²¹

$$\begin{aligned} \text{For fast pulse detector, } F_i &= \frac{p}{c_v}, \\ \text{For large area detector, } F_v &= \frac{p}{c_v \varepsilon_0 \varepsilon_r}, \\ \text{For pyroelectric point detector, } F_D &= \frac{p}{c_v \sqrt{\varepsilon_0 \varepsilon_r \tan \delta}}, \end{aligned}$$

where ε_0 is the vacuum permittivity ($8.854 \times 10^{-12}\text{ F/m}$) and c_v is the volume specific heat of the sample.

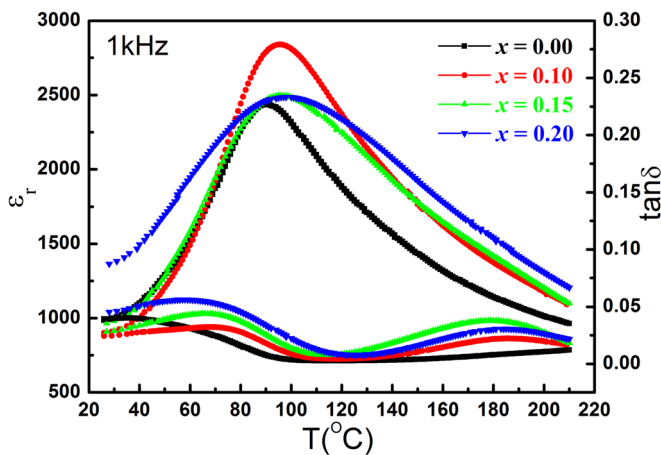


FIG. 2. Temperature-dependent dielectric constant (ε_r) and loss ($\tan \delta$) of poled CSBN(x) ceramics measured at 1 kHz.

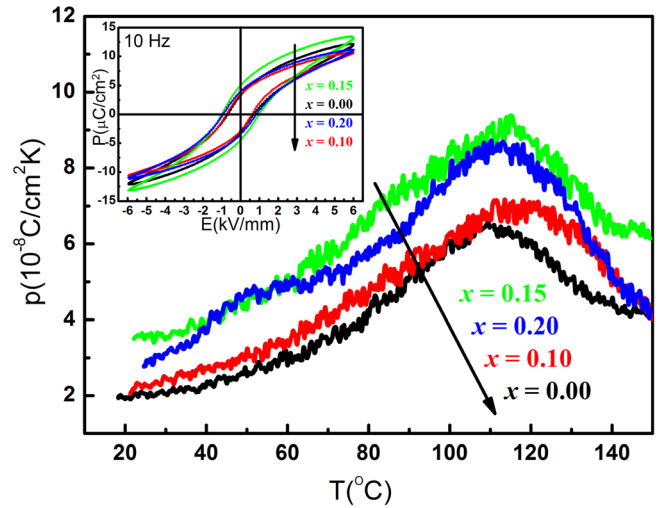


FIG. 3. Pyroelectric coefficient (p) of poled CSBN(x) ceramics as a function of temperature. The inset shows the P - E hysteresis loops of CSBN(x) ceramics measured at 10 Hz.

Table I shows the pyroelectric coefficient and FOM of the CSBN(x) ceramics. Pyroelectric properties of other lead-free materials^{2,6} are also given for comparison. As we can see, CSBN(x) samples display higher pyroelectricity when Ca-substitution occurs and achieve the highest p value of $3.61 \times 10^{-8}\text{ C/cm}^2\text{ K}$ at room temperature when $x=0.15$, which is 176% to that observed in pure SBN samples ($2.05 \times 10^{-8}\text{ C/cm}^2\text{ K}$) and much higher than that reported in Ca-doped SBNN ceramics ($1.67 \times 10^{-8}\text{ C/cm}^2\text{ K}$).¹⁷ With its low c_v and moderate ε_r , CSBN(0.15) ceramics exhibit FOMs of $F_i = 172\text{ pm/V}$, $F_v = 0.021\text{ m}^2/\text{C}$, and $F_d = 11.5\text{ }\mu\text{Pa}^{-1/2}$ at room temperature, superior to other lead-free ceramics⁶ and comparable to that published for $\text{Sr}_{0.5}\text{Ba}_{0.5}\text{Nb}_2\text{O}_6$ crystal.² The ε_r , $\tan \delta$, F_v , and F_d of CSBN(x) ceramics are also listed in Table I for comparison. Figures 4(a)–4(c) show F_i , F_v , and F_d as a function of temperature over the range of $20\text{--}80^\circ\text{C}$, respectively. It can be observed that FOMs of CSBN(0.15) are all at higher levels than other compositions. We can also find that with the benefit of low ε_r and $\tan \delta$ [Figure 4(d)], F_v and F_d of CSBN(0.15) stay high and change little with temperature over a broad range. Therefore, CSBN(0.15) ceramic can be a suitable candidate of lead free ceramics for fabrication of pyroelectric devices.

For deeply understanding of the pyroelectric effect and polarization behavior of CSBN(x) ceramics, the ferroelectric properties are further studied. The inset of Figure 3 depicts the polarization versus applied electrical field (P - E) hysteresis loops of CSBN(x) ceramics measured at 10 Hz. The maximum remnant polarization P_r ($5.16\text{ }\mu\text{C/cm}^2$), saturated polarization P_s ($13.40\text{ }\mu\text{C/cm}^2$), and coercive electric field H_c (0.967 kV/mm) have all been measured at $x=0.15$. These results are in accordance with the variation trend of pyroelectric coefficient (p) in Figure 3.

With increasing Ca content, the ferroelectric and pyroelectric properties of CSBN(x) have been enhanced followed by their subsequent reduction after reaching the maximum values at $x=0.15$. This may be related to the crystal structure modifications induced by Ca-substitution. It has been reported that the ferroelectric polarization is linearly proportional to the atomic displacement (Δz) inside the unit cell.²²

TABLE I. Pyroelectric coefficient and figures of merit of the CSBN(*x*) ceramics and other lead-free materials at room temperature.

Material	ϵ_r		$\tan \delta$		P ($\times 10^{-8}$ C/cm ² K)	c_v ($\times 10^6$ J/m ³ K)	F_i ($\times 10^{-10}$ m/V)	F_v ($\times 10^{-2}$ m ² /C)		F_D ($\times 10^{-5}$ Pa ^{-1/2})	
	1 kHz	100 Hz	1 kHz	100 Hz				1 kHz	100 Hz	1 kHz	100 Hz
$x = 0.00$	971	1024	0.039	0.033	2.05	2.10	0.98	1.14	1.08	0.53	0.56
$x = 0.10$	885	910	0.024	0.021	2.27	2.10	1.08	1.38	1.34	0.79	0.83
$x = 0.15$	933	972	0.027	0.024	3.61	2.10	1.72	2.08	2.00	1.15	1.20
$x = 0.20$	1329	1401	0.044	0.041	2.80	2.10	1.33	1.13	1.08	0.59	0.59
KNLNT ^a		1230		0.0182	1.65	2.63	0.63 ^b		0.57 ^b		0.44 ^b
BNKBT ^c		853		0.0278	3.25	2.88	1.13 ^b		1.49 ^b		0.78 ^b
SBN ^d	400		0.003		5.50	2.34	2.35	6.64		7.21	

^aModified KNN-based ceramic, [(K_{0.5}Na_{0.5})_{0.96}Li_{0.04}](Nb_{0.8}Ta_{0.2})O₃.⁶^bCalculated according to the ϵ_r , $\tan \delta$, p , and c_v value.⁶^cModified BNT-based ceramic, [Bi_{0.5}(Na_{0.95}K_{0.05})_{0.5}]_{0.95}Ba_{0.05}TiO₃.⁶^dSr_{0.5}Ba_{0.5}Nb₂O₆ single crystal.²

The appropriate substitution of smaller Ca²⁺ for Sr²⁺ and Ba²⁺ may enhance the structural distortion to some degree and result in larger Δz and thus an increase in spontaneous polarization, as stated in SCNN ceramics.¹⁶ As T_c changes little with Ca addition (Figure 2), higher Pr in CSBN(*x*) will contribute to higher p values. However, when Ca content reaches a high level (such as 0.20), the compositional fluctuations become so large that a second phase may occur. Therefore, the phase transition in CSBN(0.20) become extremely diffuse which causes much higher ϵ_r around room

temperature. The Pr and p of CSBN(*x*) ceramics also get peak value at $x = 0.15$ and then decrease with x . The abnormal pyroelectric properties in CSBN(0.20), as reflected in Figures 3 and 4, are also in accordance with the assumption.

In summary, dielectric, ferroelectric, and pyroelectric properties of CSBN(*x*) lead-free ceramics were investigated. The appropriate substitution of smaller Ca²⁺ for Sr²⁺ and Ba²⁺ may enhance the structural distortion to some degree and result in an increase in spontaneous polarization and thus pyroelectric coefficient. Hence the ferroelectric and

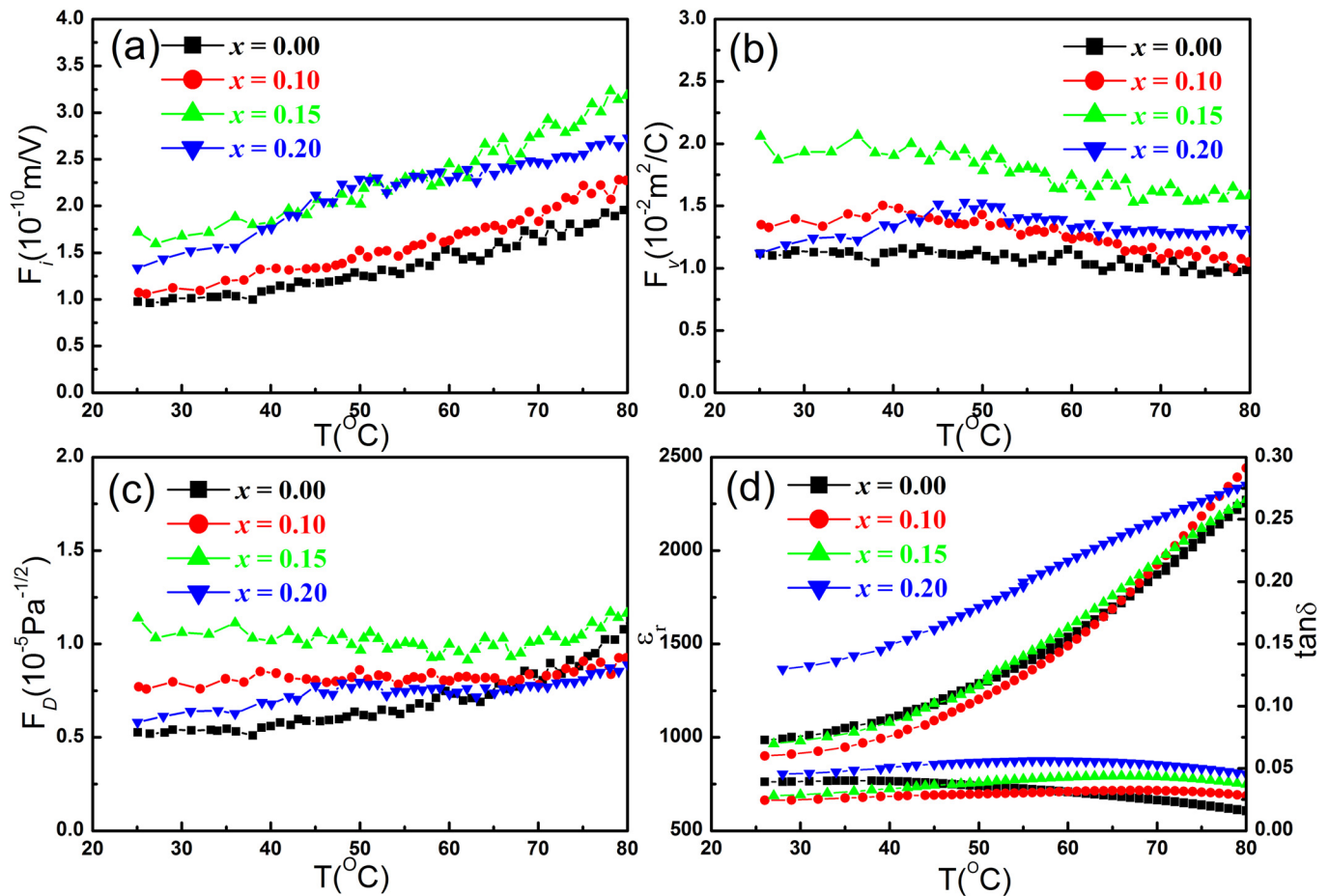


FIG. 4. (a) Figure of merit F_i , (b) figure of merit F_v , (c) figure of merit F_D , and (d) dielectric constant (ϵ_r) of CSBN(*x*) ceramics measured at 1 kHz as a function of temperature over the range of 20–80 $^{\circ}\text{C}$.

pyroelectric properties of CSBN(*x*) have been enhanced followed by subsequent reduction on the extent of Ca-substitution. Pyroelectric properties superior to other lead-free ceramics were achieved in CSBN(0.15) ceramics, with pyroelectric coefficient of $3.61 \times 10^{-8} \text{ C/cm}^2 \text{ K}$ and pyroelectric FOM of $F_i = 172 \text{ pm/V}$, $F_v = 0.021 \text{ m}^2/\text{C}$, and $F_d = 11.5 \mu\text{Pa}^{-1/2}$. These excellent properties unveil the potential of CSBN(0.15) ceramics for pyroelectric devices applications.

This work was supported by National Program on Key Basic Research Project (973 Program) (Grant No. 2012CB619406) and National Natural Science Foundation (NNSF) of China (Grant No. U0937603, 10974216 and 51002173).

- ¹A. Jahanzeb, C. M. Travers, D. P. Butler, Z. Celik-Butler, and J. E. Gray, *Appl. Phys. Lett.* **70**(26), 3495 (1997).
- ²R. W. Whatmore, *Rep. Prog. Phys.* **49**(12), 1335 (1986).
- ³L. Liu, X. Li, X. Wu, Y. Wang, W. Di, D. Lin, X. Zhao, H. Luo, and N. Neumann, *Appl. Phys. Lett.* **95**(19), 192903 (2009).
- ⁴Q. Zhang, M. Fan, S. Jiang, T. Yang, and X. Yao, *Appl. Phys. Lett.* **101**(6), 062906 (2012).
- ⁵X. Lei, X. Dong, C. Mao, Y. Chen, F. Cao, and G. Wang, *Appl. Phys. Lett.* **101**(26), 262901 (2012).

- ⁶S. T. Lau, C. H. Cheng, S. H. Choy, D. M. Lin, K. W. Kwok, and H. L. W. Chan, *J. Appl. Phys.* **103**(10), 104105 (2008).
- ⁷Y. P. Guo, M. Y. Gu, and H. S. Luo, *J. Am. Ceram. Soc.* **94**(5), 1350 (2011).
- ⁸S. B. Lang, *Ferroelectrics* **330**(1), 103 (2006).
- ⁹A. M. Glass, *J. Appl. Phys.* **40**(12), 4699 (1969).
- ¹⁰M. Venet, I. A. Santos, J. A. Eiras, and D. Garcia, *Solid State Ionics* **177**(5–6), 589 (2006).
- ¹¹A. M. Glass, *Appl. Phys. Lett.* **13**(4), 147 (1968).
- ¹²J. Zhang, G. Wang, F. Gao, C. Mao, F. Cao, and X. Dong, *Ceram. Int.* **39**(2), 1971 (2013).
- ¹³T. T. Fang and H. Y. Chung, *Appl. Phys. Lett.* **94**(9), 092905 (2009).
- ¹⁴S. N. Murty, G. Padmavathi, A. Bhanumathi, and K. L. Murty, *Phys. Status Solidi A* **128**(1), K47 (1991).
- ¹⁵T.-T. Fang and F.-Y. Chen, *J. Appl. Phys.* **100**(1), 014110 (2006).
- ¹⁶R.-J. Xie, Y. Akimune, K. Matsuo, T. Sugiyama, N. Hirotsaki, and T. Sekiya, *Appl. Phys. Lett.* **80**(5), 835 (2002).
- ¹⁷Y. B. Yao and C. L. Mak, *J. Alloys Compd.* **544**, 87 (2012).
- ¹⁸Y. J. Qi, C. J. Lu, J. Zhu, X. B. Chen, H. L. Song, H. J. Zhang, and X. G. Xu, *Appl. Phys. Lett.* **87**(8), 082904 (2005).
- ¹⁹R. R. Neurgaonkar, W. F. Hall, J. R. Oliver, W. W. Ho, and W. K. Cory, *Ferroelectrics* **87**(1), 167 (1988).
- ²⁰M. Muehlberg, M. Burianek, B. Joschko, D. Klimm, A. Danilewsky, M. Gelissen, L. Bayarjargal, G. P. Görlner, and B. O. Hildmann, *J. Cryst. Growth* **310**(7–9), 2288 (2008).
- ²¹R. W. Whatmore, *Ferroelectrics* **118**(1–4), 241 (1991).
- ²²S. C. Abrahams, S. K. Kurtz, and P. B. Jamieson, *Phys. Rev.* **172**(2), 551 (1968).